O. Etisken*¹, F. Antoniou, F. Zimmermann, CERN, Geneva, Switzerland C. Milardi, A. Desantis, LNF-INFN, Frascati, Italy

¹ also at Kirikkale University

Abstract

The current injector complex design of the FCC-ee project consists of e^+/e^- linacs, which accelerate the beams up to 6 GeV, a damping ring at 1.54 GeV, a pre-booster ring, accelerating the beam up to 16 GeV and a booster synchrotron ring integrated in the collider tunnel accelerating the beams up to the collision energies. The purpose of the damping ring is to accept the 1.54 GeV beam coming from the linac-1, damp the positron/electron beams and provide the required beam characteristics for the injection into the linac-2. In this presentation the damping ring design is introduced and analytical calculations on various collective effect such as space charge, intra-beam scattering, longitudinal micro-wave instability, transverse mode coupling instability, ion effects, electron cloud and coherent synchrotron radiation, are presented.

INTRODUCTION

The Future Circular Collider (FCC) e^+e^- project is a design study of a high-luminosity, high-energy circular electron-positron collider to be installed in a new tunnel of around 98 km circumference. It is planned to be used as a high precision machine for the investigation of the Z, W, Higgs and top particles at center of mass energies varying between 91.2 and 365 GeV [1,2].

The injector complex design of the FCC- e^+e^- consists of an e^+/e^- linac, which accelerates the beams up to 6 GeV, a pre-booster ring (PBR), accelerating the beams from 6 GeV to 16 GeV, and a booster synchrotron ring (BR), accelerating the beams up to the collision energy [3]. The pre-accelerator complex design (baseline) consists of an electron source, two linacs, a positron target and a damping ring. The 2-bunch and multi-bunches options have been discussed in the past months [4]. In this study, the collective effect estimates are done for the multi-bunches option. The ring has a racetrack shape consisting of 2 arcs and 2 straight sections; each arc has 50 FODO cells, whereas each straight section has two long damping wiggler magnets (17 m, 1.8 T) to reach short damping time [4]. The beam parameters for the multi-bunch DR design option are summarized in Table 1.

In this study, analytical estimates related to collective effects have been performed for the DR design as collective effects can be a limiting factor for the performance of an accelerator.

Table 1: Beam Parameters of the DR

Parameter	DR
Energy, E [GeV]	1.54
Circumference, C [m]	270.65
Geo. emit. (h), ϵ_x [nm·rad]	1.25
Bunch length, σ_z [mm]	3.19
Momentum sprd., σ_{δ} (×10 ⁻²)	0.074
Harmonic number, h	360
Mom. compac., α_c (×10 ⁻³)	1.49
Horizontal tune, Q_h	22.57
Vertical tune, Q_{ν}	23.61
Synchrotron tune, Q_s	0.019
Energy loss/turn, U_0 [MeV]	0.47
Chamber radius, b [m]	0.01
Bunch pop., N_b (×10 ¹⁰)	2.13
Bunch spacing, ΔT_b [ns]	18
Number of bunches, n_b	50

COLLECTIVE EFFECT ESTIMATES

Space Charge

The Space Charge (SC) effect may apply undesired effects on the beam like intensity limitation, emittance growth, tune shift [5–7]. The incoherent tune shift by space charge effect can be estimated by an analytical expression for the incoherent SC tune shift for Gaussian bunches is given by [8–10]:

$$\delta Q_{y}^{\rm inc} = -\frac{N_{b} r_{e} C}{(2\pi)^{\frac{3}{2}} \beta^{2} \gamma^{3} \sigma_{z} \sqrt{\epsilon_{y}}} \left\langle \frac{\sqrt{\beta_{y}}}{\sqrt{\beta_{x} \epsilon_{x} + D_{x}^{2} \sigma_{\delta}^{2}} + \sqrt{\epsilon_{y} \beta_{y}}} \right\rangle, \tag{1}$$

where r_e is the electron radius, C the circumference and N_b the bunch population, ϵ_x and ϵ_y the geometrical transverse emittances, D_x the horizontal dispersion and $\beta_{x,y}$ the horizontal and vertical betatron functions, respectively.

The maximum value is computed after the beam reaches the equilibrium emittance values in all planes for electron and positron beams. For the case of electron beam, $\delta Q_y^{\rm inc} = -0.09$ while for the case of the positron beam $\delta Q_y^{\rm inc} = -0.01$. For the electron beam, the values are small and thus the SC is not expected to pose a limitation with respect to transverse emittance blow up or particle losses. For the positron case, the tune shift may cause issue due to resonance crossing. Thus, it should be taken into account on the working point choice.

^{*} ozgur.etisken@cern.ch

Intra-Beam Scattering

Intra-beam Scattering (IBS) refers to the binary Coulomb scattering events between the particles within a beam, leading to the re-distribution of the phase space [5, 11, 12]. Figure 1 shows the horizontal emittance evolution during the stored time of the electron beam. The solid red line shows the emittance evaluation without IBS effect and the dashed blue line shows the emittance as taking into account the IBS effect. The calculations were done using the IBS module of MAD-X [13]. The emittance growth with respect to the natural equilibrium emittance (without IBS) at the end of the stored time is around 78% for the DR design. Although the effect seems large, the emittance including the IBS is still within the limit for the DR. The emittance growth is even smaller (6%) for the positron beam. Consequently, the IBS effect is not expected to pose a limitation for both electron and positron beams. In addition, the calculations show that if the beam is extracted at around 10 ms, it is possible to have smaller extraction horizontal emittance.

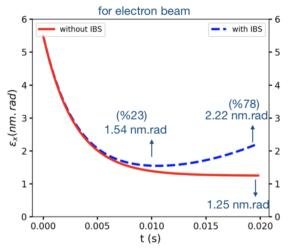


Figure 1: Emittance (hor.) evolution of the DR for electron beam. Blue line shows the emittance including IBS effect while red lines shows the emittance without IBS during the stored time.

Longitudinal Microwave Instability

The fields of ultra-relativistic particles in an accelerator interacts with the vacuum chamber and this may affect the particles behind those generating the fields which is known as wake fields. The fields may cause instabilities in longitudinal and transverse planes [5, 14]. A broad-band impedance, representing the effect of all discontinuities of the beam pipe, can cause a microwave instability. According to the Boussard criterion, the corresponding threshold impedance is given by [8, 15]:

$$\frac{Z_0^{\parallel}}{n} = Z_0 \frac{\pi}{2} \frac{\gamma \alpha_c \sigma_{\delta}^2 \sigma_z}{N_b r_e} \left(\frac{b}{\sigma_z}\right)^2, \tag{2}$$

where Z_0 is the impedance of free space. Based on the DR design parameters for electron and positron beams, the Boussard threshold impedance Z_0^{\parallel}/n was calculated at injection and at the equilibrium state. The results are summarized in Table 2. They correspond to 14 Ω and 2585 Ω for the electron and positron beam at injection, respectively. For the equilibrium state, it becomes 0.1Ω for the equilibrium state and the Boussard criterion is below than the longitudinal impedance. The longitudinal impedance is assumed as 1 Ω . If the vacuum chamber radius is increased to around 35 mm, it become 1.25 Ω which become well above than the impedance.

Transverse Mode Coupling Instability

The transverse impedance of the machine can drive the head-tail instability (HTI) and/or the transverse mode coupling instability (TMCI) [8]. The TMCI threshold for a broad-band resonator impedance is given by [8, 15]:

$$R_{\text{th}}[k\Omega/m] = \frac{0.6E[\text{GeV}]Q_sQ}{\beta_y[m]Q_b[\text{C}]\sigma_t[\text{ps}]f_r^2[\text{GHz}]},$$
 (3)

where
$$Q_b = N_b e$$
, $f_r = W_r/(2\pi)$, $W_r = c/b$, $\sigma_t = \sigma_z/c$.

The thresholds for both electron and positron beams were estimated at injection and at the equilibrium state. They correspond to 12.06 M Ω /m (for e^-) and 3.54 M Ω /m (for e^+) at injection. In addition, it becomes 3.78 M Ω /m (for $e^$ and e^+) at the equilibrium state. The transverse impedance (Z_t^{\perp}) of the DR is estimated as 0.95 M Ω /m, which is well below the calculated threshold.

Ion Effects

The ions which is created in the vacuum chamber can be trapped and accumulated by the fields of the electron beam and eventually can lead to beam instability [16–18]. The critical mass for trapping of a singly charged ion is [8,9]:

$$A_{\rm crit} \cong \frac{N_b \Delta T_b c r_p}{2\sigma_{\rm v}(\sigma_{\rm x} + \sigma_{\rm v})},\tag{4}$$

where r_p is the classical proton radius. Figure 2 shows the critical mass for the DR at injection and equilibrium state as well as the thresholds for different ions. The trapping condition is lower than almost all the possible ions' thresholds for especially injected beam. Ions trapped around the electron beam induce a tune shift, which at the end of the train is given by [8, 9, 16]:

$$\delta Q_{\rm ion} \simeq \frac{N_b n_b r_e c}{\pi \gamma \sqrt{\epsilon_x \epsilon_y}} \left(\frac{\sigma_{\rm ion} p}{k_B T} \right), \tag{5}$$

where σ_{ion} is the ionization cross section, p is the vacuum pressure, k_B is the Boltzmann constant. $\delta Q_{\text{ion}} = 0.003$ which is small at injection and it is even smaller at the equilibrium state, assuming a pressure of 10^{-9} mbar for the DR.

The accumulated ions can lead to the fast-ion instability (FII) with a rise time given by [8, 9, 16, 17]:

$$\tau_{\rm inst} \simeq \frac{0.1 \gamma \sigma_x \sigma_y}{N_b n_b c r_e \beta_y \sigma_{\rm ion}} \left(\frac{k_B T}{p}\right) \left(\sqrt{\frac{8}{\pi}}\right).$$
 (6)

MC2: Photon Sources and Electron Accelerators

licence (© 2022). Any distribution of this work must maintain

terms of the CC BY

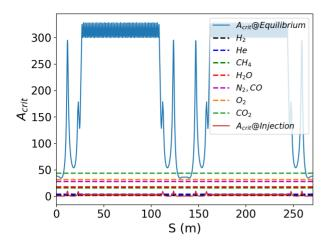


Figure 2: Critical mass for the alternative DR in comparison to the thresholds for various molecules.

The FII rise times are obtained as 770 and 14 revolution times (t_{rev}) for the injection and equilibrium parameters, respectively. Instabilities with such rise times can be compensated with a feedback system, provided that 10^{-9} mbar damping ring vacuum pressures are achieved.

Electron Cloud

Electrons present in the vacuum pipe can be trapped by the fields of the positively charged circulating particles [17, 19]. When free electrons in the vacuum chamber get accelerated in the electromagnetic field of the beam and hit the chamber walls, electron amplification can occur through the multipacting effect. The e^- build up saturates when the attractive beam field is compensated by the field of the electrons, at a neutralization density, given by [17]:

$$\rho_{\text{neutr}} = \frac{N_b}{L_{\text{sep}} \pi b_x b_y},\tag{7}$$

where L_{sep} [m] is the bunch spacing. The single bunch e^- cloud instability (ECI) occurs above the e^- density threshold estimated by [17, 20, 21]:

$$\rho_{\rm th} = \frac{2\gamma Q_s}{\sqrt{3}Qr_e\beta_{\rm v}C},\tag{8}$$

where $Q = \min(7, \frac{w_e \sigma_z}{c})$ is the angular oscillation frequency of the electrons interacting with the beam, with $w_e^2 = \frac{N_b r_e c^2}{2\sigma_z \sigma_y (\sigma_x + \sigma_y)}$. The neutralization density was calculated as $125.06 \times 10^{11} / \text{m}^3$. The neutralization density exceeds the threshold for at the equilibrium state. This should be investigated with detailed simulations (see Table 2).

Coherent Synchrotron Radiation

Coherent synchrotron radiation (CSR) occurs if the SR wavelength is comparable to the bunch length. The CSR may lead to a micro-bunching instability under the following

Table 2: Collective Effects Estimates for the DR

Parameters	DR
SC tune shift @inj. (e^{-}) (h/v)	0.004/0.003
SC tune shift @inj. (e^+) (h/v) [×10 ⁻⁴]	1.8/0.1
SC tune shift @eq. $(e^+ \text{ and } e^-)$ (h/v)	0.01/0.09
Emit. growth by IBS @inj. (e^{-}) [%]	78
Emit. growth by IBS @inj. (e^+) [%]	6
Longitudinal imp. $[\Omega]$	1
LMI th. @inj. $(e^-)[\Omega]$	14
LMI th. @inj. (e^+) [Ω]	2585
LMI th. @eq. $(e^+ \text{ and } e^-)$ [Ω]	0.1
Transverse impedance [M Ω /m]	0.95
TMCI th. @inj. (e^-) [M Ω /m]	12.06
TMCI th. @inj. (e^+) [M Ω /m]	3.54
TMCI th. @eq. $(e^+ \text{ and } e^-) [M\Omega/m]$	3.78
Chamber radius [m]	0.01
Max. tune shift by ions	0.003
FII rise time @inj./@eq.[t_{rev}]	770/14
e-cloud neutr. dens. $[10^{11}/m^3]$	125.06
ECI dens. th. @inj. $[10^{11}/m^3]$	1634
ECI dens. th. @eq. $[10^{11}/m^3]$	22.06
Stupakov parameter @eq. (Λ)	3.18
$\frac{\rho}{h}$ @eq.	0.73
$0.5 \rho \Lambda^{-3/2}$ @eq. [m]	0.65
σ_z @eq. [m]	0.003
Stupakov parameter @inj. $(e^+/e^-)(\Lambda)$	0.22/0.0001
$\frac{\rho}{h}$ @inj. (e^{+}/e^{-})	0.73
$0.5 \rho \Lambda^{-3/2}$ @inj. (e^+/e^-) [m]	33.8/>>
σ_z @inj. (e^+/e^-) [m]	0.001/0.0034

conditions [5, 22–25]:

$$\sigma_z \ge 0.5 \rho \Lambda^{-3/2}$$
 and $\frac{\rho}{h} \le \Lambda$, (9)

where b is the chamber radius, ρ the bending radius and Λ known as the Stupakov-Heifets parameter:

$$\Lambda = \frac{N_b r_e \rho \sqrt{2\pi}}{C |\alpha_c| \sigma_z \gamma \sigma_\delta^2} \tag{10}$$

The instability conditions were calculated and presented in the Table 2, showing that no CSR instability is expected.

CONCLUSION

In this study, analytical estimates of various collective effects were presented for one of the DR design options discussed during the past months. Based on these, no major limitations are expected due to IBS, TMCI and CSR. Concerning the SC, the tune shift at the equilibrium state might be an issue. Furthermore, the Boussard criterion is below the longitudinal impedance assuming a vacuum chamber radius of 10 mm. It was shown that the neutralization density

exceeds the e-cloud instability threshold for the equilibrium state. The fast rise times of the FII can be compensated with a feedback system, provided a vacuum pressure of 10^{-9} mbar are achieved for the DR.

REFERENCES

- [1] A. Abada et al. "FCC-ee: The Lepton Collider", Eur. Phys. J. Spec. Top., vol. 228, pp. 261–623, 2019. doi:10.1140/epjst/e2019-900045-4
- [2] K. Oide et al. "Design of beam optics for the future circular collider e⁺e⁻ rings", Physical Review Accelerators and Beams, vol. 19, p. 111005, 2016. doi:10.1103/PhysRevAccelBeams.19.111005
- [3] S. Ogur et al., "Overall Injection Strategy for FCC-ee", in Proc. eeFACT'18, Hong Kong, China, Sep. 2018, pp. 131. doi:10.18429/JACoW-eeFACT2018-TUPAB03
- [4] C. Milardi et al. "Progress on the damping ring and transfer lines WP4", FCC-ee Injector Design (CHART proposal) Coordination meeting 06, 28, October, 2021.
- [5] A. Wolski, "Beam Dynamics in High Energy Particle Accelerators", Imperial College Press, 2014.
- [6] M. Ferrario, M. Migliorati, and L. Palumbo. "Space Charge Effects", in *Proc. of the CAS-CERN Accelerator School: Ad*vanced Accelerator Physics, Trondheim, Norway, 19–29 August 2013, CERN-2014-009, pp.331-356.
- [7] W. T. Weng. "Space Charge Effects-Tune shifts and resonances", SLAC PUB 4058, August 1986.
- [8] G. Rumolo, J. B. Jeanneret, Y. Papaphilippou, and D. Quatraro, "Collective Effects in the CLIC Damping Rings", in *Proc. EPAC'08*, Genoa, Italy, Jun. 2008, paper MOPP049, pp. 658–660.
- [9] T. Agoh, M. Korostelev, D. Schulte, F. Zimmermann, K. Yokoya. "Collective effects in the CLIC damping rings", CERN-AB-2005-049 CLIC Note 632, 2005.
- [10] K. Schindl. "Space charge", in Proc. of CAS CERN Accelerator School: Basic Course on General Accelerator Physics, Montreux, Switzerland, 11 - 20 May 1998.
- [11] H. Wiedemann, "Particle Accelerator Physics", Springer.
- [12] F. Antoniou. "Optics Design of Intrabeam Scattering Dominated Damping Rings", CLIC Note 989, CERN-THESIS-2012-368, 2013.
- [13] CERN BE/ABP Accelerator Beam Physics Group. "Methodical Accelerator Design".

- [14] M. Ferrario, M. Migliorati, and L. Palumbo. "Wakefields and Instabilities in Linear Accelerators," in *Proc. of the CAS-CERN Accelerator School: Advanced Accelerator Physics*, Trondheim, Norway, 19–29 August 2013, CERN-2014-009.
- [15] E. Koukovini, K. S. B. Li, N. Mounet, G. Rumolo, and B. Salvant, "Impedance Effects in the CLIC Damping Rings", in *Proc. IPAC'11*, San Sebastian, Spain, Sep. 2011, paper TUPC050, pp. 1111–1113.
- [16] F. Zimmermann et al. "Experiments on the Fast Beam-Ion Instability at the ALS", SLAC-PUB-7617, October, 1997.
- [17] F. Zimmermann, "Two-Stream Effects in Present and Future Accelerators", in *Proc. EPAC'02*, Paris, France, Jun. 2002, paper THZGB001, pp. 25-29.
- [18] R. Nagaoka. "Ions", in Proc. of the CAS-CERN Accelerator School: Intensity Limitations in Particle Beams, Geneva, Switzerland, 2–11 November 2015, Vol. 3/2017, CERN-2017-006-SP.
- [19] G. Rumolo and G. Iadarola. "Electron Clouds", in Proc. of the CAS-CERN Accelerator School: Intensity Limitations in Particle Beams, Vol. 3/2017, CERN-2017-006-SP, CERN, Geneva, 2017.
- [20] E. Belli, P. Costa Pinto, G. Rumolo, T. F. Sinkovits, M. Taborelli, and M. Migliorati, "Electron Cloud Studies in FCC-ee", in *Proc. IPAC'18*, Vancouver, Canada, Apr.-May 2018, pp. 374–377. doi:10.18429/JACoW-IPAC2018-MOPMK012
- [21] K. Ohmi and F. Zimmermann, "Study of coherent tune shift caused by electron in positron storge rings", *in Proc. of second Asian Particle Accelerator Conference*, in *Proc. APAC'01*, Beijing, China, Sep. 2001, paper WEP056, pp. 445–447.
- [22] G. Stupakov and S. Heifets. "Beam instability and microbunching due to coherent synchrotron radiation", *Physical Review Special Topics-Accelerators and Beams*, vol. 5, p. 054402, 2002. doi:10.1103/PhysRevSTAB.5.054402
- [23] G. Stupakov and S. Heifets. "Beam instability and microbunching due to coherent synchrotron radiation", SLAC-PUB-8761, 2001.
- [24] Cheng-Ying Tsaiy. "Suppressing CSR Microbunching in Recirculation Arcs", in *Proc. IPAC'18*, Vancouver, Canada, Apr.-May 2018, pp. 1784–1789. doi:10.18429/ JACOW-IPAC2018-WEYGBE1
- [25] F. Zimmermann. "Estimates of CSR Instability Thresholds for Various Storage Rings", ATS-Note-2010-049, CLIC-Note-861.